A SIMPLE MODEL OF EARTH'S MAGNETIC FIELD REVERSALS

Frank Stefani, Gunter Gerbeth, and Uwe Günther

1. Introduction

There is ample paleomagnetic evidence that the Earth's magnetic field has reversed its polarity many times. The mean rate of reversals varies from nearly zero during the so-called superchrons to approximately 5 per Myr in the present. Many observations suggest a distinct asymmetry of reversals with the decay being much slower than the following recreation of the dipole with opposite polarity [1,2]. Observational data also indicate a possible correlation of the field intensity with the interval between subsequent reversals [2,3]. A third hypothesis concerns the bimodal distribution of the Earth's virtual axial dipole moment (VADM) with two peaks at approximately 4 x 10^{22} Am^2 and at twice that value [4]. Although these reversal features are still controversially discussed, it is worthwhile to ask how they could be reflected by dynamo theory.

In a series of recent papers [5,6,7], we have analysed a simple mean-field dynamo model with a spherically symmetric helical turbulence parameter α with regard to the appearance of typical reversal features. Surprisingly, all of them turned out to be explainable by the peculiar magnetic field dynamics in the vicinity of an exceptional point of the spectrum of the non-selfadjoint dynamo operator where two real eigenvalues coalesce and continue as a pair of complex conjugate eigenvalues [8]. This exceptional point is typically associated with a nearby local maximum of the growth rate dependence on the magnetic Reynolds number. It is the negative slope of this curve between the local maximum and the exceptional point that makes stationary dynamos vulnerable to some prevailing noise. This way, the system can leave a (quasi-)stable state towards the exceptional point and beyond into the oscillatory branch where the polarity transition occurs. An apparent weakness of this reversal model, the necessity to fine-tune the magnetic Reynolds number and/or the radial profile $\alpha(r)$ in order to adjust the operator spectrum in an appropriate way, was overcome in [6]. For strongly supercritical dynamos we identified a general tendency of the exceptional point and the associated local maximum to move close to the zero growth rate line were the indicated reversal scenario can be actualised. In [7] we compared paleomagnetic data of five recent reversals with typical numerical time series resulting from our model. It was shown that it is again the strong super-criticality of the considered dynamo models that may explain the typical time scales of the observed asymmetric reversals.

In the present report we give an overview about our recent activities towards a better understanding of geomagnetic polarity reversals.

2. The model

We consider a simple mean-field dynamo model with a spherically symmetric, isotropic helical turbulence parameter α. The induction equation for the magnetic field $\mathbf{B}$ reads

$$\frac{\partial \mathbf{B}}{\partial \tau} = \nabla \times (\alpha \mathbf{B}) + \frac{1}{\mu_0 \sigma} \Delta \mathbf{B} \quad , \tag{1}$$

with magnetic permeability μ_0 and electrical conductivity σ. For the Earth's outer core we will assume the magnetic diffusion time $\tau_{diff} = \mu_0 \sigma R^2$ to be ~200 kyr. The divergence-free magnetic field $\mathbf{B}$ can be decomposed into a poloidal and a toroidal component, according to $\mathbf{B} = -\nabla \times (\mathbf{r} \times \nabla S) - \mathbf{r} \times \nabla T$. The defining scalars S and T are expanded in spherical harmonics of degree l and order m with expansion coefficients $s_{l,m}(r,\tau)$ and $t_{l,m}(r,\tau)$. For the envisioned spherically symmetric and isotropic α^2 dynamo model, Eq. (1) decouples for each degree l and order m into the following pair of equations:

$$\frac{\partial s_{l,m}}{\partial \tau} = \frac{1}{r}\frac{\partial^2}{\partial r^2}(r s_{l,m}) - \frac{l(l+1)}{r^2} s_{l,m} + \alpha(r,\tau) t_{l,m} \tag{2}$$

$$\frac{\partial t_{l,m}}{\partial \tau} = \frac{1}{r}\frac{\partial}{\partial r}\left[\frac{\partial}{\partial r}\left(r t_{l,m}\right) - \alpha(r,\tau)\frac{\partial}{\partial r}\left(r s_{l,m}\right)\right] - \frac{l(l+1)}{r^2}\left[t_{l,m} - \alpha(r,\tau) s_{l,m}\right] \quad . \tag{3}$$

The boundary conditions read $\partial s_{l,m} / \partial r \,|_{r=1} + (l+1) s_{l,m}(1) = t_{l,m}(1) = 0$. In the following we consider only the axial dipole field with $l = 1$ and $m = 0$ and will henceforth use the shorthand notation $s := s_{1,0}$ and $t := t_{1,0}$.

We will focus on a particular kinematic radial profile $\alpha_{kin}(r) = 1.916 \cdot C \cdot (1 - 6r^2 + 5r^4)$, which is characterized by a sign change along the radius.. Our main motivation for this choice is that quite similar profiles had been shown to exhibit oscillatory behaviour [9]. As was shown in [10], such sign changing α profiles seem indeed to be relevant for the Earth's outer core. Under the influence of the self-excited magnetic field the kinematic α profile must be reduced (or "quenched", which is the common notion in dynamo theory) in order to ensure saturation of the dynamo process. We assume here a special algebraic quenching by the magnetic field energy density, averaged over spherical angles, which can be expressed by $E_{mag}(r,\tau) = 2r^{-2} s^2(r,\tau) + r^{-2}(\partial(r s(r,\tau))/\partial r)^2 + t(r,\tau)$. In addition to this quenching, the $\alpha(r)$ profiles are perturbed by radial profiles of noise which are considered constant within a certain correlation time τ_{corr}. Physically, such a noise term can be interpreted as a consequence of changing boundary conditions for the flow in the core, but also as a substitute for the omitted influence of higher multipole modes on the dominant axial dipole mode. In summary, the time dependent profile $\alpha(r,\tau)$ entering Eqs. (2,3) is written as

$$\alpha(r,\tau) = \frac{1.916 \cdot C \cdot (1 - 6r^2 + 5r^4)}{1 + E_{mag}(r,\tau)/E_0} + \xi_1(\tau) + \xi_2(\tau) r^2 + \xi_3(\tau) r^3 + \xi_4(\tau) r^4 \quad , \tag{4}$$

with the noise correlation given by $\langle \xi_i(\tau) \xi_k(\tau + \tau_1) \rangle = D^2 \cdot (1 - |\tau_1| / \tau_{corr}) \cdot \Theta(1 - |\tau_1| / \tau_{corr}) \delta_{ik}$. C is the magnetic Reynolds number, D is the noise strength, and E_0 measures the mean magnetic energy density. The equation system (2-4) is time-stepped by means of an Adams-Bashforth method.

3. Numerical results

In order to understand the asymmetry of reversals and the correlation of field strength with interval duration, we start with the noise-free case. Figure 1 shows the magnetic field

evolution according to the equation system (2-4) for D=0 and different dynamo numbers C. The critical value of C for the onset of dynamo action is 6.78. The nearly harmonic oscillation for C=6.8 becomes more and more saw-tooth shaped for increasing C, with a clear asymmetry between the slow field decay and the fast field recreation during the reversal. At C=7.24 a transition to a steady dynamo has occurred.

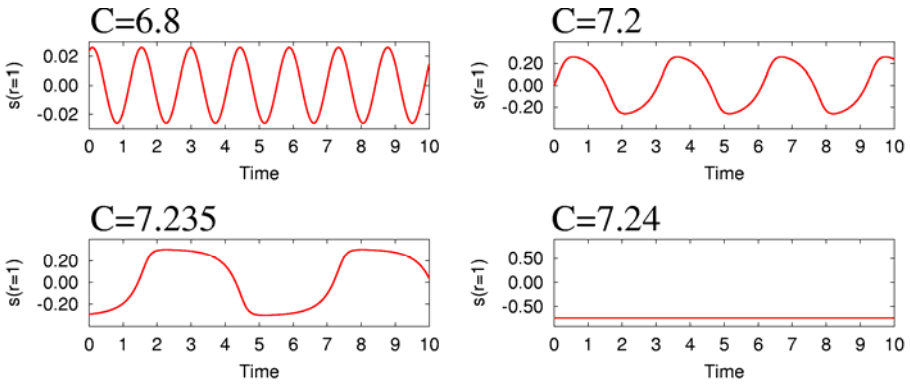

Fig. 1: Magnetic field evolution for the noise free case D=0.

In Fig. 2 we examine in detail the evolution of the magnetic field within approximately half a period of the anharmonic oscillation for the particular value C=7.237 that is only slightly below the transition from oscillatory to steady behaviour. Figure 2a shows the time dependence of the poloidal field component at the surface of the core, $s(r=1)$, during this half period, with the typical slow decay and the fast recreation of the field. This behaviour is analysed in detail at 9 selected instants τ_i (i=1...9) for which the corresponding quenched profiles $\alpha(r,\tau_i)$ (Fig. 2c) and the instantaneous fields $s(r,\tau_i)$ (Fig. 2d) are depicted. We see in Fig. 2c that $\alpha(r)$ undergoes only slight changes during the anharmonic oscillation and that it comes very close to the unquenched, kinematic $\alpha_{kin}(r)$ (denoted by K) when the magnetic field is small in the middle of the reversal (approximately at instants 5 and 6).

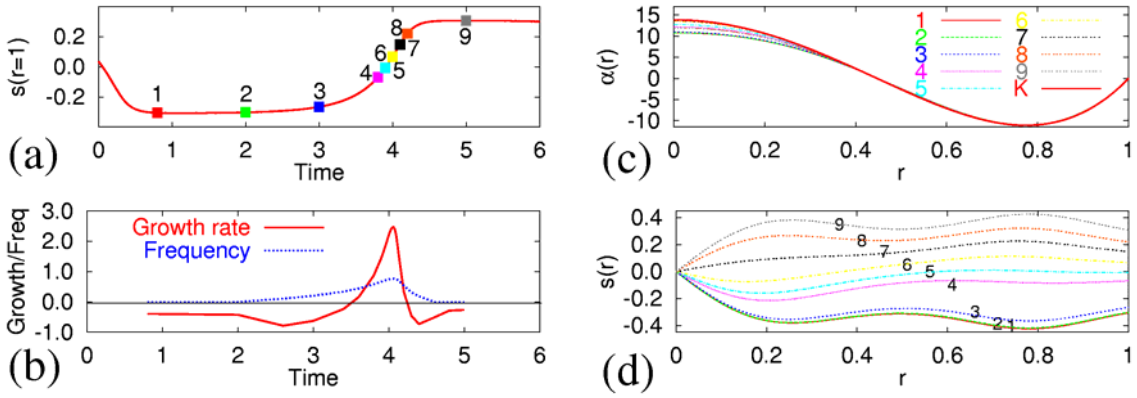

Fig. 2: Explanation of the field dynamics for C=7.237 and D=0.

To understand this sort of relaxation oscillation better, it is instructive to plug the instantaneous $\alpha(r,\tau_i)$ profiles into an eigenvalue solver (for which the time derivatives on the left hand sides of Eqs. (2) and (3) are replaced by $\lambda\, s(r)$ and $\lambda\, t(r)$, respectively, with $\lambda = p + 2\pi i f$). Figure 2b shows the resulting instantaneous growth rates p and the

instantaneous frequencies f during the half-oscillation. Evidently, the reversal starts with a very slow field decay (slightly negative p) which, however, accelerates itself and drives the system into an oscillatory behaviour (f becomes non-zero within $2.0 < \tau < 4.5$). Near $\tau = 4$, when the quenching of α is weak, the instantaneous growth rate reaches rather high values. Later we will see that for strongly supercritical dynamos these high growth rates result in a field dynamics that is much faster than what would be expected from the diffusion time-scale.

It is instructive to look not only on the time sequence of instantaneous eigenvalues as we did in Fig. 2b, but to identify the position of these eigenvalues relative to the exceptional point of the spectrum of the dynamo operator. For the considered C=7.237, we analyse in Fig. 3a the growth rates for the profiles $\alpha(r,\tau_i) = 1.916 \cdot C \cdot C^* \cdot (1 - 6r^2 + 5r^4)/(1 + E_{mag}(r,\tau_i)/E_0)$, where the additional scaling factor C^* has been introduced in order to identify the position of the eigenvalue (at the dashed vertical line C^*=1) relative to the exceptional points E_i. At the exceptional point E_k of the kinematic $\alpha_{kin}(r)$, the first eigenvalue branch K1 coalesces with the second branch K2 and both continue as a pair of complex conjugate eigenvalues. For all other curves (i=1...9), only the exceptional points are indicated by E_i whereas the branches of the second eigenvalue have been omitted. In this framework, a reversal can be described as follows: At the instant 1, the slightly negative growth rate p is located close to the maximum of the non oscillatory branch. The resulting slow field decay accelerates itself, since the system moves down (instant 2) from the maximum of the real branch towards the exceptional point. Then the system enters the oscillatory branch (3-7). Finally the system moves back again (8,9) but with opposite polarity.

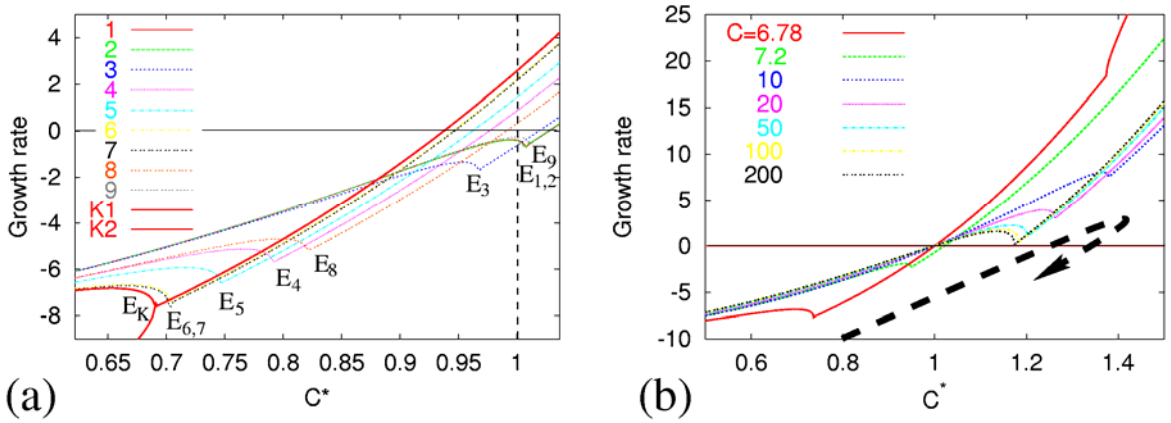

Fig. 3: The role of exceptional points for the understanding of reversals. (a) Growth rate dependence on C for the kinematic profile and for the quenched $\alpha(r,\tau_i)$ profiles. (b) Growth rates for the saturated α profiles with C=6.78, 7.2, 10, 20, 50, 100, 200.*

The transition point between oscillatory and steady dynamos (C=7.239) is characterized by the fact that the maximum of the non-oscillatory branch crosses the zero growth rate line. Beyond this point, the field is growing rather than decaying, leading to a stable fixed point somewhere to the left of the maximum of the non-oscillatory branch, and hence to a non-oscillatory dynamo (cf. the case C=7.24 in Fig. 1). If noise comes into play it will soften the sharp border between oscillatory and steady dynamos. This means, in particular, that even above the transition point, the noise can trigger a jump to the right of the maximum from where the described reversal process can start (Fig. 2).

Having identified the exceptional point and the nearby local maximum as the spectral features that are responsible for both the slow decay before and the fast recreation of the field after the polarity transition, one may ask now why the operator of the actual geodynamo should possess just such a special spectrum. A possible answer to this question was given in [6] and is illustrated in Fig. 3b. Roughly speaking, highly supercritical dynamos (with $C>>C_{\mathrm{crit}}$) have a tendency to saturate in a state for which the exceptional point and its associated local maximum are situated close to the zero growth rate line. Interestingly, this happens independently on whether the exceptional point for the original $\alpha_{kin}(r)$ profile was above the zero growth rate line or below it. Our example belongs to the second type. Starting from the kinematic $\alpha_{kin}(r)$ (C=6.78), for which the exceptional point is well below the zero line, it rises rapidly above zero to a maximum value, but for even higher C it moves back towards the zero line.

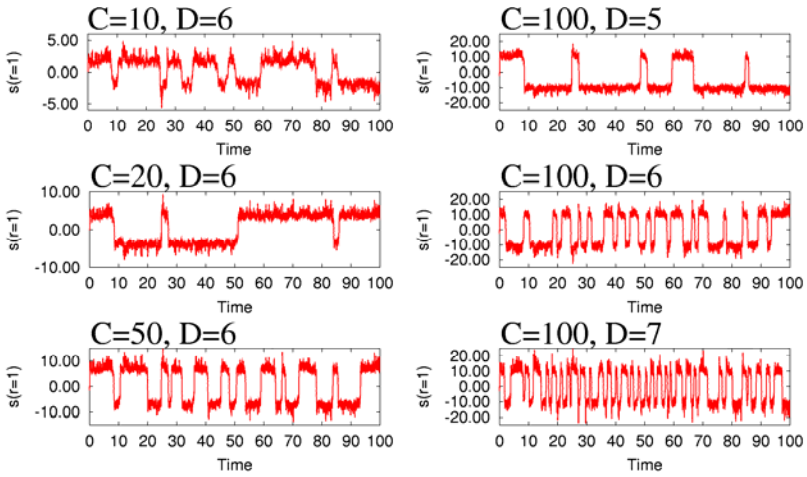

Fig. 4: Time series of the magnetic field for varying magnetic Reynolds numbers C and noise strengths D.

Without noise (D=0) and for C>7.239, the position of the local maximum above the zero growth rate line leads to a steady dynamo. The presence of noise will sometimes bring the actual growth rate below zero, and then the indicated reversal process can start. A number of time series for different values of C and D is depicted in Fig. 4.

4. Comparison with paleomagnetic data

In this section we will validate if our model can explain real paleomagnetic data. For this purpose we have used recently published material about five reversals which occurred during the last two million years [3]. In Fig. 5a we show the virtual axial dipole moment (VADM) during the 80 kyr preceeding and the 20 kyr following a polarity transition for five reversals from the last 2 million years, and their average. In all five individual curves, as well as in their averages, the asymmetry of the reversal process is clearly visible. The dominant features are a field decay over a period of 50-80 kyr and a rather sharp recreation of the field with opposite polarity within 5-10 kyr.

It has been an old-standing puzzle to explain in particular this fast recreation when a diffusive timescale of 200 kyr has to be taken into account. A possible solution of this problem is to assume a turbulent resistivity which is much larger than the molecular resistivity. However, this assumption which is hardly justified by physical arguments is by no means necessary to explain the asymmetry. Figure 5b exhibits the average curve of Fig. 5a together with four

average curves resulting from our numerical simulations. Apart from the only slightly super-critical case C=8, D=1, which provides a much too slow magnetic field evolution, the other examples with C=20, 50, 100 and D=6 show very realistic time series with the typical slow decay and fast recreation. As noted above, the fast recreation results from the fact that in a small interval during the transition the dynamo operates with a nearly unquenched $\alpha(r)$ profile which yields, in case that the dynamo is strongly supercritical, rather high growth rates.

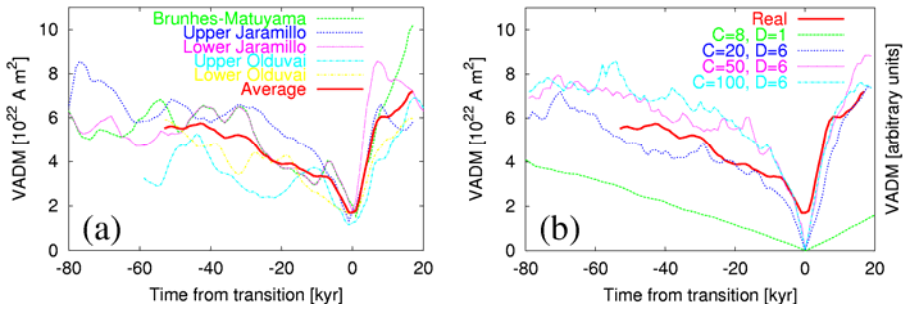

Fig. 5: Comparison of paleomagnetic reversal data (a) and numerically simulated ones (b).

5. Outlook

We have shown that a simple spherically symmetric α^2 dynamo model exhibits a number of features which are typical for Earth's magnetic field reversals, in particular an asymmetric shape. As it does not include the necessary North-South asymmetry of α we cannot claim that our model is an appropriate model of the geodynamo. Nevertheless, since the basic mechanism is not restricted to the particular mean-field model, it should be possible to identify it also in more realistic dynamo models.

References

[1] J.-P. Valet, L. Meynadier (1993), Geomagnetic field intensity and reversals during the past 4 million years, Nature, 366, 238

[2] J.-P. Valet, L. Meynadier (2005), Geomagnetic dipole strength and reversal rate over the past two million years, Nature, 435, 802

[3] J. A. Tarduno, R. D. Cottrell, A. V. Smirnov (2001), High geomagnetic intensity during the mid-Cretaceous from Thellier analyses of single plagioclase crystals, Science, 291, 1779

[4] R. Heller, R. T. Merrill, P. L. McFadden (2003), The two states of paleomagnetic field intensities for the past 320 million years, Phys. Earth Planet. Inter. 135, 211

[5] F. Stefani, G. Gerbeth (2005), Asymmetric polarity reversals, bimodal field distribution, and coherence resonance in a spherically symmetric mean-field dynamo model, Phys. Rev. Lett. 94, Art. No.184506

[6] F. Stefani, G. Gerbeth, U. Günther, M. Xu (2006), Why dynamos are prone to reversals, Earth Planet. Sci. Lett. 143, 828

[7] F. Stefani, G. Gerbeth, U. Günther (2006), A paradigmatic model of Earth's magnetic field reversals (2006), Magnetohydrodynamics, in press

[8] T. Kato, Perturbation theory of linear operators, Springer, Berlin, 1966

[9] F. Stefani, G. Gerbeth (2003), Oscillatory mean field dynamos with a spherically symmetric, isotropic helical turbulence parameter α, Phys. Rev. E 67, Art. No. 027302

[10] A. Giesecke, U. Ziegler, G. Rüdiger (2005), Geodynamo alpha-effect derived from box-simulations of rotating magnetoconvection, Phys. Earth Planet. Int. 152, 90